Noncollinear magnetic ground state of PrFeAsO

2011 EPL 93 17003

(http://iopscience.iop.org/0295-5075/93/1/17003)

A Letters Journal Exploring the Frontiers of Physics

January 2011

EPL, **93** (2011) 17003
doi: 10.1209/0295-5075/93/17003

www.epljournal.org

Noncollinear magnetic ground state of PrFeAsO

J. Liu[1], B. Luo[1], R. Laskowski[2] and K. L. Yao[1,3(a)]

[1] *School of Physics, Huazhong University of Science and Technology - Wuhan 430074, China*
[2] *Technische Universität Wien - Getreidemarkt 9/165TC, A-1060 Vienna, Austria, EU*
[3] *International Center of Materials Physics, The Chinese Academy of Science - Shengyang 110015, China*

received 13 April 2010; accepted in final form 18 December 2010
published online 28 January 2011

PACS 74.25.Jb – Electronic structure (photoemission, etc.)
PACS 74.70.Dd – Ternary, quaternary, and multinary compounds (including Chevrel phases, borocarbides, etc.)

Abstract – Noncollinear magnetic investigations of the ground state in PrFeAsO have been performed by the density-functional theory. We calculated the total energy and made structure optimization, and the electronic density of states of PrFeAsO was analyzed. There are three different magnetic structures in PrFeAsO defined by experiments. Based on these magnetic structures, we studied four collinear and four noncollinear cases. The ground state is found to take the ordering proposed by Zhao, in which the FeAs plane is of stripe antiferromagnetism and Pr spins are perpendicular to Fe spins. The electronic density of states indicates that for PrFeAsO the increase of the electron Coulomb interaction leads to a decrease in conductivity.

Antiferromagnetism is relevant to high-temperature superconductivity because copper oxide and iron arsenide superconductors arise from electron- or hole- doping of their antiferromagnetic parent compounds [1,2]. If magnetism is important for the superconductivity of these materials, it is essential to get the correct magnetic ground state of their parent compounds. The neutron powder diffraction has defined the crystal structure and the magnetic ordering of the RFeAsO system, which shows a structural phase transition from tetragonal to orthorhombic with decreasing temperature [3–8]. However, it is found that at very low temperature there exits strong magnetic coupling between the rare-earth elements, and they form antiferromagnetic ordering in the RO layer, meanwhile their spins are coupled with iron spins. The Fe spin structure is supposed to be the same as that arranged above the magnetic phase transition temperature when data fitting. Hence it needs more investigations to help define the iron spins ordering and the rare-earth element spin ordering in the ground state.

PrFeAsO is one parent compound of the iron arsenide family, and it has a transition temperature of up to 52 K with oxygen partially replaced by fluorine. Three groups have worked on determining the magnetic structure of PrFeAsO and their results are totally different. First, Kimber *et al.* proposed the collinear magnetic model, where both Fe and Pr spin ordering are within the *ab*-plane in the two-left, one-right magnetic structure [5]. According to Kimber's structure, we constructed two kinds of collinear solutions CM1 and CM2. Pr spins are aligned antiferromagnetically along the *b*-axis in the CM1 solution (see fig. 1(a)) and are aligned ferromagnetically in the CM2 solution (fig. 1(b)). Simultaneously a rather complicated noncollinear magnetic structure was shown by Zhao *et al.* [6], where the Pr spins align along the *c*-axis, trios of spins are coupled ferromagnetically, and adjacent trios align antiferromagnetically. This noncollinear magnetic structure is called NCM1 in our work (fig. 1(c)). Finally, Maeter *et al.* reported a new noncollinear magnetic structure different to NCM1, which is called NCM2 [7]. In NCM2 Pr spins order within the *ab*-plane and Fe spins make an acute angle with the *ab*-plane (fig. 1(d)).

The two-dimensional electronic structure in the iron-arsenide compound has been analyzed by many groups, but there are few reports about the three-dimensional electronic-structure calculations including the rare-earth magnetic-moment direction. With the unconstrained method, we defined the Pr spin ordering and Fe spin ordering in the ground state. The lattice parameters were taken from refs. [6,9], and we made a $\sqrt{2} \times \sqrt{2} \times 1$ supercell.

All calculations were performed by the WIENNCM code [10,11], the Perdew-Burke-Ernzerh of 96 GGA

(a) E-mail: klyao@hust.edu.cn

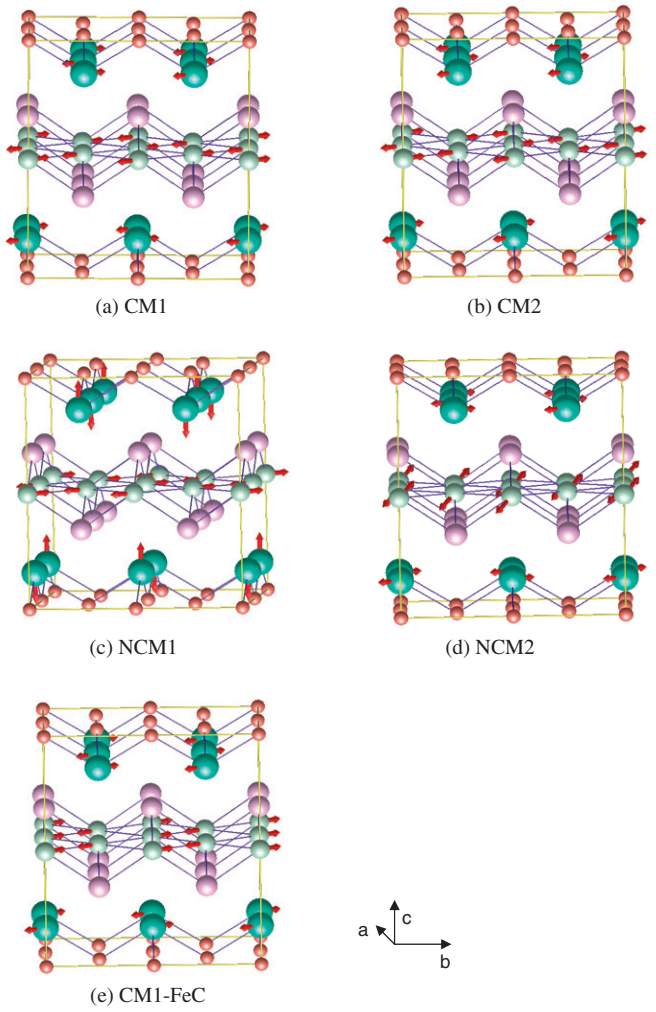

Fig. 1: (a) (Colour on-line) The collinear magnetic structure of the CM1 case; (b) the CM2 case; (c) the noncollinear magnetic structure of NCM1 case; (d) the NCM2 case; (e) the CM1-FeC case. The red arrows indicate the magnetic-moment directions of the magnetic ions. Light-green balls indicate Fe ions, green balls indicate Pr ions, red balls indicate O ions and purple balls indicate As ions.

exchange-correlation potential was used. Atomic sphere radii were set to 2.04, 2.39, 2.12 and 2.30 a.u. for O, Fe, As and Pr, respectively. We used a $4 \times 4 \times 4$ k-point sampling of the Brillouin zone. The unconstrained approach was adopted in order to lower the total energy and optimize the magnetic structure. The $RK_{\max}$ value was set to 7.0. Within GGA+U calculations, the effective Coulomb interaction value was set to 2 eV, 4 eV and 5 eV for Fe ions and 4 eV, 6 eV and 7 eV for Pr ions, respectively [12]. Energy convergence and charge convergence were attained by $10^{-5}e$.

The two interpenetrating square antiferromagnetic orderings (checkboard ordering and stripe ordering) in the FeAs plane have been proposed by theoretical works, for the Fe-Fe effective nearest-neighbor and next-nearest-neighbor magnetic interactions are comparable to each other [13–15]. The stripe antiferromagnetic ordering is observed by experiments [16–18]. In order to compare with experiments and other theoretical work, we also considered the checkboard antiferromagnetic ordering. We used checkboard ordering instead of stripe ordering in the above four solutions and got the corresponding solutions of CM1-FeC, CM2-FeC, NCM1-FeC and NCM2-FeC. (The magnetic structure of CM1-FeC is similar to CM1, but the FeAs plane takes a checkboard ordering, see fig. 1(e).) Only two kinds of antiferromagnetic ordering are discussed in the NCM structure, for the experiments and previous theoretical calculations both indicate antiferromagnetic ordering is more stable than other orderings (ferromagnetic, nonmagnetic and paramagnetic) [19,20].

Table 1 gives the energy of each configuration. The energy value in the CM1 case is set to zero; the other cases are given as the energy differences relative to the CM1 case (energy values reserve four decimal places). From table 1, it can be seen that two kinds of noncollinear magnetic models are more stable than the collinear magnetic models. When the Coulomb repulsion is considered into Pr and Fe ions, NCM1 is the ground state and NCM2 is the metastable state. On three different on-site Coulomb interactions, NCM1 keeps the lowest energy. In NCM1 the Fe spin shows stripe antiferromagnetic ordering within the *ab*-plane and the Pr spin plane is perpendicular to the Fe spin plane. Both NCM1 and NCM2 are noncollinear three-dimensional magnetic structures. Moreover the energy results indicate that in noncollinear magnetic structure the stripe ordering is more stable than the checkboard ordering, because the NCM1 case and NCM2 case have lower energy than the NCM1-FeC case and NCM2-FeC case, respectively. If the Coulomb repulsion is not considered, NCM2 takes the lowest energy. The X-ray absorption (XAS) and resonant inelastic X-ray scattering (RIXS) for 122 and 1111 Fe pnictides show qualitative similarity to the Fe metal, therefore the cases which included Coulomb interaction are in accord with the actual conditions [12,21].

Using the unconstrained approach, the magnetic structure can be optimized according to the charge density. The orientation of the spins is described using spherical coordinates. Each magnetic moment is symbolized by a vector $\vec{R}(\rho, \theta, \varphi)$, so that θ corresponds to the angle in the basal plane, and φ is the angle relative to the c-axis (z-direction). In the optimization of the magnetic structure, Pr spins and Fe spins are found to make small changes in θ but give a relative large deflection in φ. The modification for θ is no more than $\pm 0.5^\circ$, this means that the magnetic ordering is quite stable within the *ab*-plane. Table 2 lists the average φ deflection angles (between ρ- and c-axis) in CM1, NCM1 and NCM2. From table 2 we can see that the NCM1 case almost keeps the original magnetic structure after optimization: both in GGA and GGA+U, Pr deflection is no more than $\pm 2^\circ$ and Fe deflection is no more than $\pm 1^\circ$. A larger alteration occurred to the NCM2 case: within GGA, φ deflection of Pr spin up to $\pm 11.5^\circ$

Table 1: Energies for each configuration of PrFeAsO. The unit of the energy is Ry.

	Energy (Ry)			
	Fe $U-J=0$ Pr $U-J=0$	$U-J=2\,\text{eV}$ $U-J=4\,\text{eV}$	$U-J=4\,\text{eV}$ $U-J=6\,\text{eV}$	$U-J=5\,\text{eV}$ $U-J=7\,\text{eV}$
CM1	0.0000	0.0000	0.0000	0.0000
CM1-FeC	0.0500	0.1011	0.0182	0.0961
CM2	−0.0005	0.1409	0.0067	0.1200
CM2-FeC	0.0419	0.1374	0.0492	0.0536
NCM1	0.0117	−0.0732	−0.0644	−0.0857
NCM1-FeC	0.0510	0.0271	0.0311	0.0502
NCM2	−0.0026	−0.0394	−0.0136	−0.0165
NCM2-FeC	0.0114	0.1212	0.0546	0.0912

Table 2: Optimization results of magnetic structure: the average φ deflection angles in the CM1 case, NCM1 case and NCM2 case.

	The average φ deflection angles (°)			
Model	Fe $U-J=0$ Pr $U-J=0$	$U-J=2\,\text{eV}$ $U-J=4\,\text{eV}$	$U-J=4\,\text{eV}$ $U-J=6\,\text{eV}$	$U-J=5\,\text{eV}$ $U-J=7\,\text{eV}$
CM1-Fe	±0.19	±0.15	±0.35	±0.16
CM1-Pr	±9.27	±5.72	±2.66	±5.66
NCM1-Fe	±0.29	±0.05	±0.62	±0.06
NCM1-Pr	±1.53	±0.02	±0.05	±0.06
NCM2-Fe	±3.40	±0.40	±0.08	±0.10
NCM2-Pr	±11.5	±5.66	±5.13	±5.36

and Fe deflection is ±3.4°; within GGA+U, Pr deflection is between ±5.66° and ±5.13°, Fe deflection is between ±0.4° and ±0.08°. It tells us Pr spins are straying from the *ab*-plane and approaching the *c*-axis, and the trend is weakened with the increase of the electronic correlations. The same tendency is also found in the CM1 case. For this reason, the optimization results prove that the NCM1 magnetic model is more stable than others. Within the GGA+U method we get Fe and Pr moments of about $2.83\,\mu_\text{B}$/Fe and $1.96\,\mu_\text{B}$/Pr using the experimental lattice. The calculated Fe moments do not reduced in noncollinear magnetic calculation or spin orbital coupling compared with other people's work [22–26].

We also performed the volume optimization, this time the spin direction of Pr and Fe were constrained. There are two cases: 1) without considering on-site Coulomb interaction, 2) with $U_\text{eff}=2\,\text{eV}$ for the Fe ion and $U_\text{eff}=4\,\text{eV}$ for the Pr ion. When the on-site Coulomb interaction is not included, the lowest total energy occurs at about $V/V_\text{exp}=5\%$, the lattice parameters are obtained with $a=8.738\,\text{Å}$ $b=8.081\,\text{Å}$ $c=8.080\,\text{Å}$. If the effective Coulomb interaction are set to 2 eV and 4 eV for Fe and Pr ions, respectively, the structure can be stabilized in $V/V_\text{exp}=9\%$ by the lattice parameters $a=8.848\,\text{Å}$ $b=8.183\,\text{Å}$ $c=8.182\,\text{Å}$. Additionally, the Fe magnetic moment is sensitive to the Fe-As bonds, with Coulomb interaction the Fe moment is $2.59\,\mu_\text{B}$ and $2.99\,\mu_\text{B}$ for 4.41 a.u. and 4.69 a.u. Fe-As bonds, respectively [27–29]. However the Pr moment keeps $1.90\,\mu_\text{B}$ during the increase of volume and it is not sensitive to the Pr-O bonds. Figure 2 illustrates the optimized results of energy and moment.

Finally, the electronic density of states (DOS) of the NCM1 case is given (see fig. 3). In fig. 3, PrFeAsO indicates the metallic property within GGA; the Fe 3*d* band and Pr 4*f* band are continuous across the Fermi level. While within GGA+U, the Fe 3*d* band and Pr 4*f* band split and move away from the Fermi level, the distance between the split bands and the Fermi level depends on the effective Coulomb repulsion value. The results of the DOS are in agreement with other theoretical calculations [20,30,31], which perform the electronic-structure calculation for PrFeAsO within LDA or GGA. If the electronic correlations are weak enough in Fe ions, the FeAs plane will be metallic or easily conductive in the excited state [21]. CM1, CM2, NCM2 and NCM1 have a similar DOS under one Coulomb interaction, that is to say, the Pr spin direction does not much affect the density of states at the Fermi level. In fig. 3(a), Fe has a few similar peaks with Pr between –2 eV and 2 eV, hence there exits a magnetic coupling between the FeAs plane and the PrO plane. We believe that the magnetoelastic

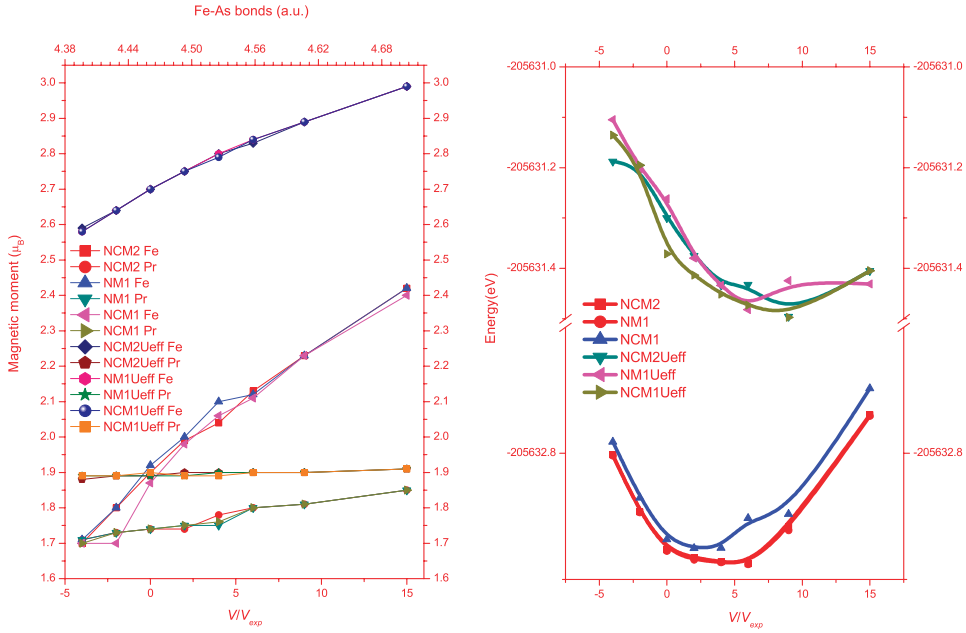

Fig. 2: (Colour on-line) The energy and magnetic moment for volume optimization.

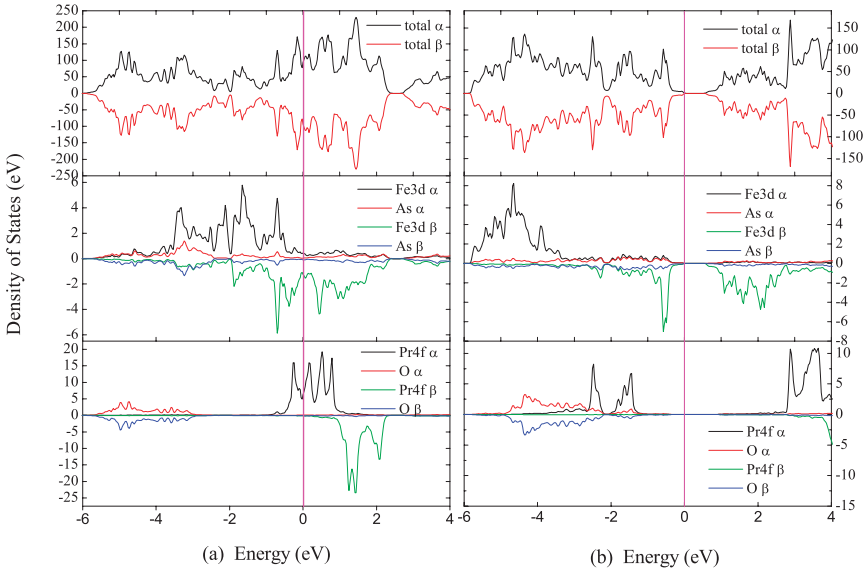

Fig. 3: (Colour on-line) Density of states of the NCM1 case. (a) The DOS without Coulomb interaction. (b) The DOS with Coulomb interaction ($U - J = 2\,\text{eV}$ for Fe and $U - J = 4\,\text{eV}$ for Pr).

volume effect reported in ref. [5] originates from both Pr spin density waves and Fe spin density waves. The superconducting isotropy of $PrFeAsO_{1-y}$ suggests a quasi–three-dimensional electronic structure in this layered superconductor, electronic-structure calculations confirm it also has a three-dimensional magnetic structure [32].

In conclusion, this work has investigated four collinear and four noncollinear magnetic structures in PrFeAsO. Total energy calculation, magnetic structure optimization and volume optimization define the magnetic ground state NCM1 in which the Pr spin is perpendicular to the Fe spin and the FeAs plane takes stripe antiferromagnetic ordering. Another noncollinear magnetic structure NCM2 is considered for metastable states. We found that the Pr spin direction does not much affect the density of states at the Fermi level. The Fe magnetic moment is sensitive to the Fe-As bonds but the Pr moment is not sensitive to the Pr-O bonds. The conductivity of PrFeAsO is mainly depending on the electronic correlation interaction, if the electronic correlations are weak enough, the PrFeAsO will show metallic character or semi-metallic character.

* * *

This work is supported by the National Natural Science Foundation of China under the Grant No. 11074081, and the Research Fund for the Doctoral Program of Higher Education of China No. 20090142110063. The data were carried out using the High Performance Computing Center experimental testbed in SCTS/CGCL.

REFERENCES

[1] Kamihara Y., Watanabe T., Hirano M. and Hosono H., *J. Am. Chem. Soc.*, **130** (2008) 3296.
[2] Wen H. H., Mu G., Fang L., Yang H. and Zhu X. Y., *EPL*, **82** (2008) 17009.
[3] Zhao J., Huang Q., de la Cruz C., Li S., Lynn J. W., Chen Y., Green M. A., Chen G. F., Li G., Li Z., Luo J. L., Wang N. L. and Dai P. C., *Nat. Mater.*, **7** (2008) 953.
[4] Qiu Y., Bao W., Huang Q., Yildirim T., Simmons J. M., Green M. A., Lynn J. W., Gasparovic Y. C., Li J., Wu T., Wu G. and Chen X. H., *Phys. Rev. Lett.*, **101** (2008) 257002.
[5] Kimber S. A. J., Argyriou D. N., Yokaichiya F., Habicht K., Gerischer S., Hansen T., Chatterji T., Klingeler R., Hess C., Behr G., Kondrat A. and Büchner B., *Phys. Rev. B*, **78** (2008) 140503(R).
[6] Zhao J., Huang Q., de la Cruz C., Lynn J. W., Lumsden M. D., Ren Z. A., Yang J., Shen X. L., Dong X. L., Zhao Z. X. and Dai P. C., *Phys. Rev. B*, **78** (2008) 132504.
[7] Maeter H., Luetkens H., Pashkevich Y. G., Kwadrin A., Khasanov R., Amato A., Gusev A. A., Lamonova K. V., Chervinskii D. A., Klingeler R., Hess C., Behr G., Büchner B. and Klauss H.-H., *Phys. Rev. B*, **80** (2009) 094524.
[8] Chen Y., Lynn J. W., Li J., Li G., Chen G. F., Luo J. L., Wang N. L., Dai P., de la Cruz C. and Mook H. A., *Phys. Rev. B*, **78** (2008) 064515.
[9] Quebe P., Terbüchte L. J. and Jeitschko W., *J. Alloys Compd.*, **302** (2000) 70.
[10] Laskowski R., Madsen G. K. H., Blaha P. and Schwarz K., *Phys. Rev. B*, **69** (2004) 140408(R).
[11] Blaha P., Schwarz K., Madsen G. K. H., Kvasnicka D. and Luitz J., *WIEN2k, An Augmented Plane Wave Plus Local Orbitals Program for Calculating Crystal Properties* (Vienna University of Technology, Austria) 2001.
[12] Anisimov V. I., Korotin D. M., Korotin M. A., Kozhevnikov A. V., Kunes J., Shorikov A. O., Skornyakov S. L. and Streltsov S. V., *J. Phys.: Condens. Matter*, **21** (2009) 075602.
[13] Klauss H. H., Luetkens H., Klingeler R., Hess C., Litterst F. J., Kraken M., Korshunov M. M., Eremin I., Drechsler S. L., Khasanov R., Amato A., Hamann-Borrero J., Leps N., Kondrat A., Behr G., Werner J. and Büchner B., *Phys. Rev. Lett.*, **101** (2008) 077005.
[14] Yildirim T., *Phys. Rev. Lett.*, **101** (2008) 057010.
[15] Dong J., Zhang H. J., Xu G., Li Z., Li G., Hu W. Z., Wu D., Chen G. F., Dai X., Luo J. L., Fang Z. and Wang N. L., *EPL*, **83** (2008) 27006.
[16] Clarina de la Cruz, Huang Q., Lynn J. W., Li J., Ratcliff II W., Zarestky J. L., Mook H. A., Chen G. F., Luo J. L., Wang N. L. and Dai P. C., *Nature*, **453** (2008) 899.
[17] Hu W. Z., Dong J., Li G., Li Z., Zheng P., Chen G. F., Luo J. L. and Wang N. L., *Phys. Rev. Lett.*, **101** (2008) 257005.
[18] Zhao J., Adroja D. T., Yao D. X., Bewley R., Li S., Wang X. F., Wu G., Chen X. H., Hu J. P. and Dai P. C., *Nature Mater.*, **5** (2009) 555.
[19] Wojdet J. C., Moreira I. de P. R. and Illas F., *J. Am. Chem. Soc.*, **131** (2009) 906.
[20] Alyahyaei H. M. and Jishi R. A., *Phys. Rev. B*, **79** (2009) 064516.
[21] Yang W. L., Sorini A. P., Chen C. C., Moritz B., Lee W.-S., Vernay F., Olalde-Velasco P., Denlinger J. D., Delley B., Chu J.-H., Analytis J. G., Fisher I. R., Ren Z. A., Yang J., Lu W., Zhao Z. X., Van den Brink J., Hussain Z., Shen Z.-X. and Devereaux T. P., *Phys. Rev. B*, **80** (2009) 014508.
[22] Xu G., Ming W., Yao Y., Dai X., Zhang S. C. and Fang Z., *EPL*, **82** (2008) 67002.
[23] Mazin I. I. and Schmalian J., *Physica C*, **469** (2009) 614.
[24] Zhang H. J., Xu G., Dai X. and Fang Z., *Chin. Phys. Lett.*, **26** (2009) 017401.
[25] Dai X., Fang Z., Zhou Y. and Zhang F. C., *Phys. Rev. Lett.*, **101** (2008) 057008.
[26] Yi W., Sun L., Ren Z., Lu W., Dong X., Zhang H. J., Dai X., Fang Z., Li Z., Che G., Yang J., Shen X., Zhou F. and Zhao Z. X., *EPL*, **83** (2008) 57002.
[27] Kasinathan D., Ormeci A., Koch K., Burkhardt U., Schnelle W., Leithe-Jasper A. and Rosner H., *New J. Phys.*, **11** (2009) 025023.
[28] Wang G. T., Qian Y., Xu G., Dai Xi. and Fang Z., *Phys. Rev. Lett.*, **104** (2010) 047002.
[29] Vildosola V., Pourovskii L., Arita R., Biermann S. and Georges A., *Phys. Rev. B*, **78** (2008) 064518.
[30] Nekrasov I. A., Pchelkina Z. V. and Sadovskii M. V., *JETP Lett.*, **87** (2008) 560.
[31] Pourovskii L., Vildosola V., Biermann S. and Georges A., *EPL*, **84** (2008) 37006.
[32] Kubota D. and Ishida T., arXiv:arXiv:0810.5623 (2008).